Anisotropic Zero Index Material: A Method of Reducing the Footprint of Vivaldi Antennas in the UHF Range

Ada-Simona Popescu[1, *], Igor Bendoym[2], Taulant Rexhepi[1], and David Crouse[3]

Abstract—In this work, an anisotropic zero index material is designed for use in Vivaldi antennas. The metasurface structures are placed within the aperture of a Vivaldi antenna to improve the directivity and gain of the emitted radiation. The range of operation is in the ultrahigh frequency (UHF) range, between 300 MHz and 3 GHz. Two approaches are presented: a type of resonant metallic metamaterial that belongs to the larger class of anisotropic zero index metamaterials and a non-resonant material. A technique for lowering the dimensions of the resonant metamaterial unit cell is presented and applied. The work presented consists of simulation results obtained with HFSS modelling software from ANSYS.

1. INTRODUCTION

Metamaterials [1] are man-made materials, engineered such that they produce specific, well-defined interactions with the electromagnetic fields. While there exists a certain amount of ambiguity when defining metamaterials, for example when it comes to including photonic crystals in the metamaterials category, the particular class of materials used in this work is represented by a periodic array composed of the so-called meta-atoms. The meta-atoms are within the periodic unit cells of the material and are the substitute for atoms and molecules within natural materials. The physical size of the meta-atoms is much smaller than the wavelength of the electromagnetic wave that excites the material. The general consensus is that the unit cell should be approximately $\lambda/10$, where λ is the wavelength of the field. Just like natural materials are characterized by macroscopic material properties, metamaterials are characterized by effective material properties. In electromagnetics, the pertinent material properties are the dielectric permittivity and the magnetic permeability, therefore, when characterizing an electromagnetic metamaterial, one has to derive its effective dielectric permittivity and magnetic permeability.

Zero index materials (ZIM) [2] are a class of materials for which one or both of the effective material parameters, dielectric permittivity and magnetic permeability can be zero. In certain applications, for instance antenna research, even though the effects of such ZIM materials are desired, they produce an unwanted impedance mismatch in the system. Another class of materials has evolved in order to address this problem: anisotropic zero index materials (AZIM). In this work, a design of such an AZIM is presented, as well as its application in antenna design. The application is a Vivaldi antenna with a coplanar design. Vivaldi antennas have a number of advantages that make them very attractive for many RF applications: they can be easily fabricated with PCB fabrication methods, and they have a high directivity and hence gain. These characteristics, along with their compact design makes them particularly suitable for antenna arrays [3]. This antenna, also called notch antenna, was introduced by Gibson in 1979 [4].

2. METAMATERIAL DESIGN: RESONANT METALLIC MATERIAL

In a broad sense, metamaterials can be defined as engineered materials, composed of building units or blocks, in the same fashion as natural materials are composed of atoms. It is often the case where the metamaterial building block is a metallic resonating structure. They can however be non-resonating, and such a design will be presented in a later section. The motivation to design and fabricate such materials is to achieve material properties otherwise unattainable with naturally occurring materials.

With the constant need for miniaturization and simple, practical solutions to radiation control, the class of two dimensional metamaterials has evolved. This class of metamaterials has the advantage of ease of integration in existing and new devices and systems.

In antenna research, a type of material that has gained a lot of interest isZIMs, for which one or both of the defining material parameters (electric permittivity ε or the magnetic permeability μ) is equal to zero. Forcing these parameters to become null produces extraordinary electromagnetic properties, such as antenna directivity enhancement. The associated disadvantage is that an impedance mismatch is produced that often offsets most or all of the improvements produced by the ZIM. This drawback led to the development of a related class of materials, anisotropic zero index metamaterials. Like natural anisotropic materials, these have one or both material parameters represented by a tensor: only one component of the tensor is to be null, and the others are non-zero, such that impedance matching conditions are satisfied.

The goal of this work was to design an isotropic zero index material that improves the directivity of the Vivaldi antenna. Two designs are presented: a resonant metamaterial, composed of metallic unit cells, and in a later section a new possible approach is presented, a non-resonant metamaterial.

First we describe the basic unit cell, a meander line resonator [5] depicted in Fig. 1 that served as starting point. We then describe the steps taken to modify this structure in order to adapt it for the particular application for this work. In its basic design, the meander line resonator was used and analyzed in numerous papers [5–7]; below, we describe a particular implementation that we adapted for our work. This procedure was described, in lesser detail, in [8], also work done in our group. The design tool used was HFSS software from Ansys.
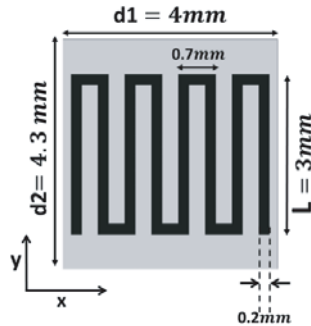

Figure 1. Meander line structure: Metal is depicted in color black and the substrate is in light grey; $d1$ and $d2$ are the dimensions of the unit cell and L is the length of the meander arm.

The meander line resonator is in essence an electrically small antenna, often used in telecommunications. A resonant material is, implicitly from definition, characterized by the resonant frequency of the particular structure. The operation range of such resonant material is rather small. Like for all metallic resonators, the dimensions of the structure determine its frequency of resonance. A common approach to design a metamaterial is to first model the infinitely periodic structure, and then model the finite-sized structure (i.e., a repeating array of what is shown in Fig. 1). The infinitely periodic structure is often a close approximation to the behavior of the finite structure and much faster to numerically model. In order to model an infinitely periodic structure in HFSS, Floquet ports at the input and output are used, and master/slave conditions for the rest of the boundaries of the air box containing the unit cell.

In order to explore the anisotropic characteristic of the material, the unit cell is analyzed for the case when the electric field is polarized parallel along the x axis, and then modeled with the electric field polarized along the y axis. For each of these cases, effective material parameters can be derived using a retrieval algorithm described in [9]. The 2 cases are illustrated below, in the Fig. 2. As one can observe, the electric field intensity is concentrated in different parts of the structure, depending on the polarization of the electric field. For reasons which will be described in the following paragraphs, the operation frequency of the meander resonator, $f_{operation}$ is not its resonant frequency but rather a higher frequency.
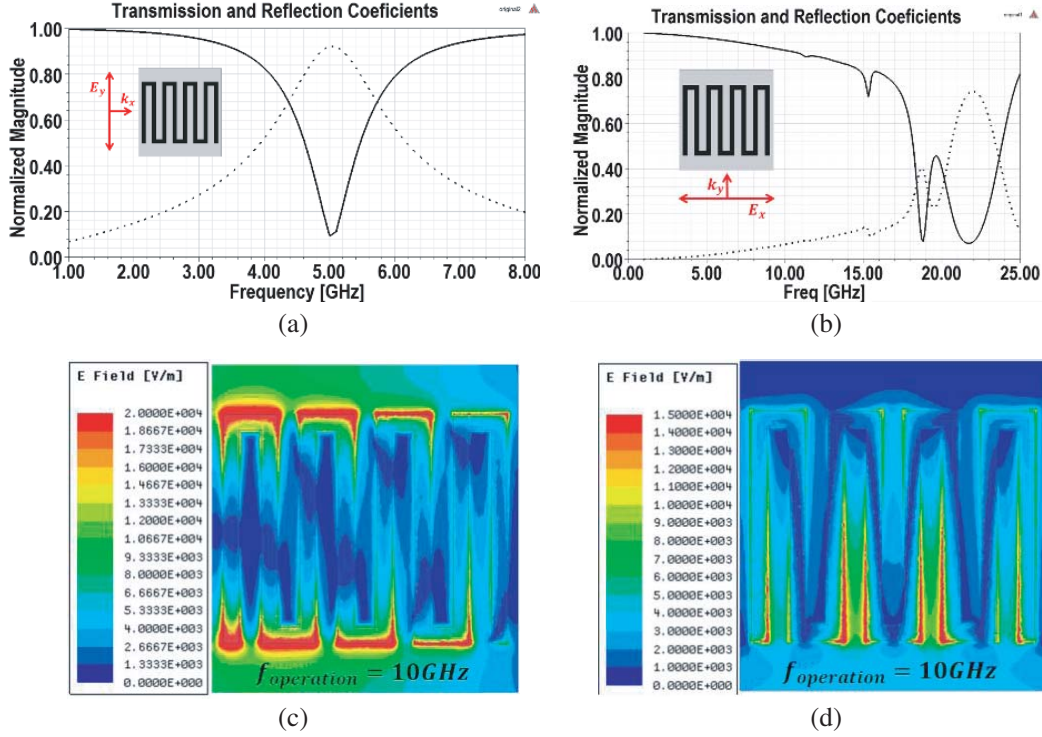

Figure 2. Transmission (solid line) and reflection (dashed line) coefficients over a wide frequency range and the electric field profiles at the frequency of operation: (a) Coefficients for the E_y polarization, where the electric field is polarized along the arms of the meander; (b) Coefficients for the E_x polarization, where the electric field is polarized perpendicular to the arms of the meander; (c) Field profile at the $f_{operation} = 10$ GHz for polarization described in (a) shows a concentration of the field in the connecting segments between the arms of the meander and in (d) field profile at the $f_{operation}$ for polarization described in (b) shows a concentration of the field in the the arms of the meander.

To illustrate a more general case, suppose a wave linearly polarized, with electric field in the xy plane, travelling from left to right, at a random orientation, as depicted in Fig. 3(a). The goal is to improve directivity, or in other words to achieve a plane wave at the exit of the metamaterial for a random polarization at input. Therefore, the utility of this metamaterial is to force all or most the radiation to propagate in the forward $\hat{x}$ direction. In terms of vector mathematics, in general, for an isotropic material:

$$k = \frac{2\pi}{\lambda_{eff}} = \frac{2\pi}{\lambda_0/n} = \frac{2\pi n}{\lambda_0} = \frac{2\pi\sqrt{\varepsilon}}{\lambda_0} \tag{1}$$

For an anisotropic material, with different permittivity in the $\hat{x}$ and $\hat{y}$ directions, the k vector has 2 components, k_x and k_y:

$$k_x = \frac{2\pi}{\lambda_{eff,x}} = \frac{2\pi}{\lambda_0/n} = \frac{2\pi n}{\lambda_0} = \frac{2\pi\sqrt{\varepsilon}_y}{\lambda_0} \tag{2}$$

$$k_y = \frac{2\pi}{\lambda_{eff,y}} = \frac{2\pi}{\lambda_0/n} = \frac{2\pi n}{\lambda_0} = \frac{2\pi\sqrt{\varepsilon}_x}{\lambda_0} \qquad (3)$$

where ε_x is the dielectric permittivity component of the tensor corresponding to the case when the electric field is polarized along the $\hat{x}$ direction, and ε_y is the dielectric permittivity component of the tensor corresponding to the case when the electric field is polarized along the $\hat{y}$ direction. In order to have all radiation to propagate in the forward $\hat{x}$ direction, the k_y component of the wave vector has to be zero. This is the same as having the x component of the permittivity, ε_x, equal to zero.

The effective material properties of the metamaterial composed of meander resonator unit cells are derived for the above described two cases. Hence, it is easy to understand that the effective material parameters are ε_x and μ_z in the case when the electric field is polarized in the x direction and ε_y and μ_z when the electric field is polarized in the y direction.

HFSS simulations provided the transfer matrix S parameters, transmittance and reflectance-parameters that are used as inputs for the retrieval algorithm described in [9]. The algorithm is applied for both cases, delivering therefore all components of the dielectric permittivity ε and magnetic permeability μ tensors. The curves over the frequency range of interest are depicted in Fig. 3 for all components of the tensors. Magnetic permeability component μ_z appears just once because in both cases H is polarized in the z direction, and, as expected, the μ_z looks practically the same.
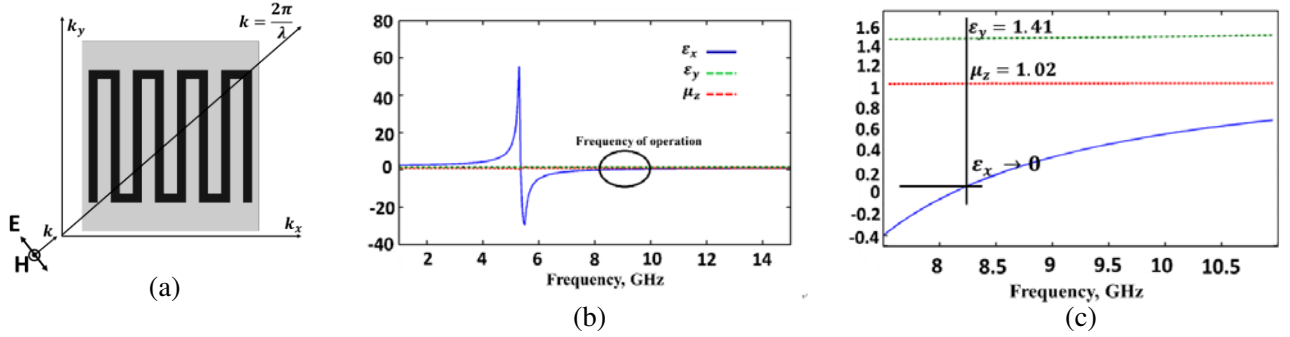

Figure 3. (a) The geometry of unit cell represented by a meander line resonator with general direction for k propagation vector; (b) The retrieved material parameters, ε_x, ε_y and μ_z; (c) A zoomed-in view of the frequency range of interest.

Since the goal is to minimize $\varepsilon_{\mathbf{x}}$ while keeping a reasonable impedance matching, we have to choose an interval where all the components have desired values. Impedance matching is mathematically expressed by the equation:

$$Z_{\mathbf{wave}} = \eta_{free\ space} \qquad (4)$$

where $Z_{\mathbf{wave}} = \sqrt{\frac{\mu_z}{\varepsilon_y}}$ is the impedance of the wave in the metamaterial region and $\eta_{free\ space} = 1$. In order to satisfy this condition, μ_z and ε_y should be as close in values as possible. It is important to note that, as expected, the resonant frequencies of the material parameters have sharp peaks and/or dips at the same frequencies as corresponding peaks and/or dips in the reflection and transmission, calculated by the HFSS software, as depicted in Fig. 2.

2.1. Methods of Minimizing the Footprint Metamaterial Unit Cell

From this point on, the challenge was to work in a much lower frequency range while keeping the dimensions of the metamaterial as small as possible. As it is well-known, the dimensions of the metallic resonators and antennas are related to their operation frequency range. Working in a lower frequency range, hence a larger wavelength, entails increased dimensions, or footprint. In order to keep the footprint at a minimum, different strategies were applied, presented in the following paragraphs.

(i) *Increase dielectric permittivity*: A common strategy to keep the footprint small, unrelated to the geometry of the metallic parts, is to increase the dielectric permittivity of the substrate. While

this is acceptable for the application, the Vivaldi antenna, it is not a convenient solution for the metamaterial, considering the fact that the antenna and metamaterial share the same substrate. In order to lower the operation frequency interval of the resonator unit cell, the resonant frequency has to be decreased, since we are working at frequencies higher than the resonant frequencies, in the spectrum, as depicted in Fig. 3(b). While increasing the dielectric permittivity of the substrate decreases the resonant frequency of the meander for one direction of the polarization, (when electric field is polarized along the x direction) it is not beneficial for the complementary polarization. If electric field is polarized along y direction, the dielectric constant component ε_y also increases, leading to impedance mismatch.

(ii) *Increase number of meanders*: The meander structure is a resonant antenna, for which the resonant frequency depends on the inductance L and capacitance C. Given that the meander line antenna is in essence a compact version of a linear dipole antenna, it is easy to deduce that increasing both the number of meander and the length of the arms will decrease the resonant frequency. Increasing the number of meanders leads to an increased inductance [5], therefore the resonant frequency decreases, which corresponds to a decrease in resonant frequency of the ε_x parameter. This is illustrated in Fig. 4(b).

(iii) *Increase length of arms*: By increasing the length of the meander line (Lm) the capacitive coupling between the neighboring unit cells is increased, leading therefore to a lower resonant frequency. Another step taken in order to keep the footprint small was to reduce the thickness of the lines. This step is illustrated in Fig. 4(c).

(iv) *Meanders within meanders (MwM)*: Since the resonant frequency that resulted after all these changes was not in accordance with the specifications, an additional step had to be taken. Based on the same rationale, that a bended wire will produce a resonator with a smaller footprint, meanders were added on the interior arms of the structure, like depicted in Fig. 5. These interior meander increase the inductance, hence the resonant frequency decreases.

(v) *Decrease length of interior meanders*: The exterior arms of the resonator are relevant only for the capacitance between adjacent unit cells. Therefore, meanders on those arms are not wanted. This coupling capacitance plays an important role in the overall resonant frequency of the metamaterial. It is beneficial to reduce the length of the interior meanders in order to reduce the metal/substrate ratio, metal being the main source for electromagnetic signal loss (i.e., absorption).

(vi) *Produce cuts to lower effective dielectric permittivity*: As it was described before, the tensor component ε_y must stay as close as possible to either a unity value, or to a value close to magnetic permeability μ_z. Parameter ε_y is affected by the coupling capacitance between unit cells along the

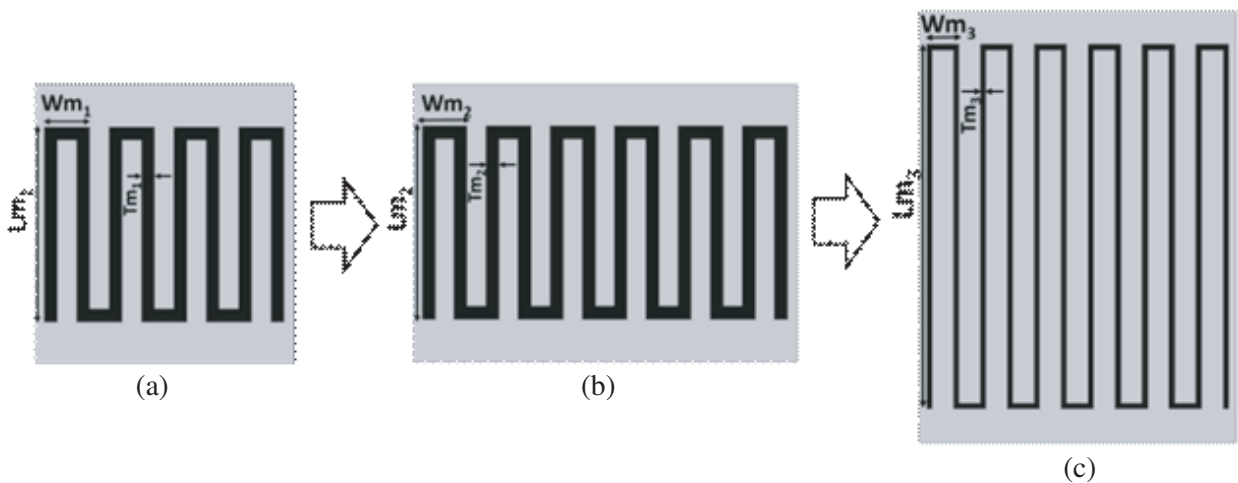**Figure 4.** Progression of meander design: $Lm1 = Lm2 < Lm3$, $Wm1 = Wm2 < Wm3$, $Tm1 = Tm2 > Tm3$. The resonant frequencies follow the relationship: $\omega1 < \omega2 < \omega3$.
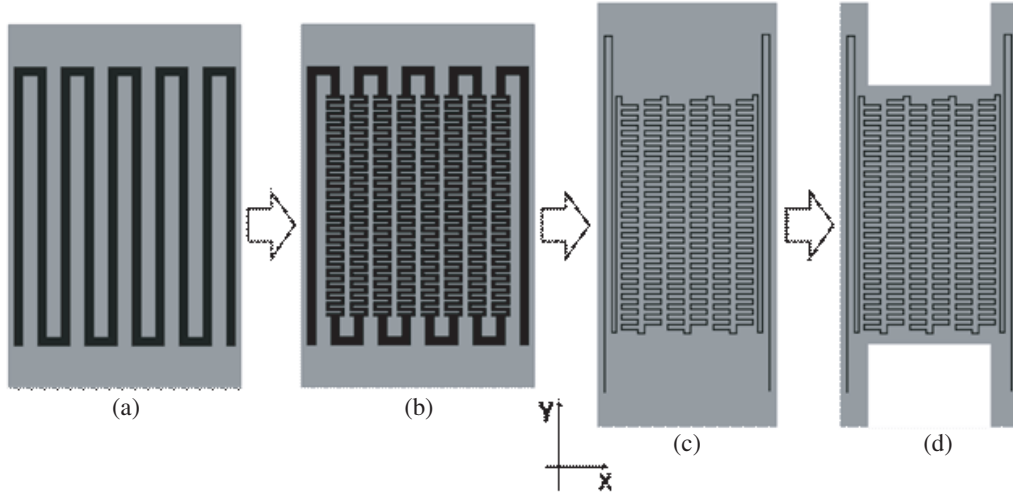
Figure 5. Progression of meander design: (a) Simple meander structure; (b) "Meanders within meander" (MwM) structure; (c) MwM optimized structure such that $\omega 1 < \omega 2 < \omega 3$; (d) MwM structure with cuts in the dielectric material, in order to optimize component ε_y of the dielectric tensor.
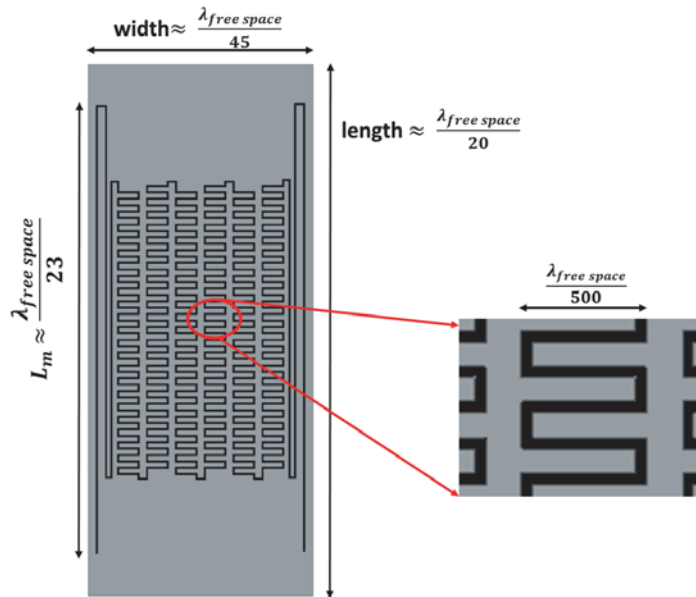

Figure 6. MwM (meanders with meanders) structure with dimensions relative to the free space wavelength of operation: Unit cell dimensions and important dimensions of the metallic part of the structure.

x directions: in order to reduce effective dielectric permittivity in that direction, cuts can be made in the material. The simulation have shown a good improvement due to this step, illustrated in Fig. 5(d).

A closer view to the meanders within meanders (MwM) final structure is shown in Fig. 6. The dimensions of the unit cell of the MwM structure relative to the free space wavelength of operation are: width $\approx \frac{\lambda_{free\ space}}{45}$, length $\approx \frac{\lambda_{free\ space}}{20}$. The length of the exterior arm of the meander is kept to a maximum possible, because this contributes to the coupling capacitance between adjacent unit cells. This capacitance is a desired effect, since the goal of this design is to lower the operation frequency of the metamaterial, and in order to do this, the resonant frequency needs to be lowered.
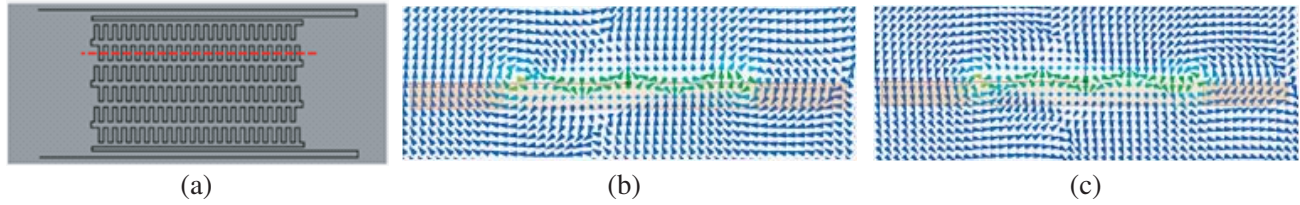
Figure 7. The electromagnetic field interactions with the MwM structure: (a) Cross section line. The magnetic field is depicted in (b) and (c) for two different phases, opposite by 180°.

An analytical approach was not fully developed at this point. Part of the research efforts were geared towards creating a lumped circuit model for associated with the MwM structure. Due to the very small size of the meanders, the development of an effective model was not possible. A future in depth analysis, aided by lumped circuit programming tools such as SPICE or MATLAB Simulink, will lead to such a model.

A qualitative understanding was developed by observing closely the fields and their interactions with the structure. The interior meanders reduce the resonant frequency of the MwM structure by increasing the local magnetic field. This is shown in Fig. 7. The green colored arrows show an enhancement of the magnetic field in the regions of the interior meanders. Due the very small size of the meanders relative to the free space wavelength of operation, a very finemesh was needed for the HFSS simulations. Further analysis is needed in order to develop an appropriate analytical approach.

3. APPLICATION: VIVALDI ANTENNA WITH A COPLANAR DESIGN

The antenna was designed based on a coplanar design, with specific targets for bandwidth, length and width. While a textbook recipe for the design of a Vivaldi antenna doesn't exist, different methods can be applied. The approach taken in this work was to first design the feed of the antenna, also called balun, and then optimize key parameters in the antenna geometry, namely the length, width and curvature of the taper [10]. The feed of the antenna is the limiting factor for the antenna bandwidth, between $f_{low,\ free\ space}$ and $f_{high,\ free\ space}$, therefore the balun has be broadband. The chosen design of the balun was a microstrip-to-slotline transition and the methodology was based on the method proposed by Zinieris et al. [11], which is based on the work of Shuppert [12] on microstrip to slotline transitions. A return loss below $-15\,\mathrm{dB}$ was achieved. Further on, the parameters investigated were the width of the antenna and the curvature of the taper, for a fixed antenna length. The antenna width has an impact on the return loss and hence on the bandwidth of the antenna. Simulations have shown that the optimum return loss was obtained in the case when the width of the antenna was of the maximum allowed value. The tapering of the metallic flares is governed by the equation:

$$y = ae^{\alpha x} + b \tag{5}$$

$$a = \frac{y_2 - y_1}{e^{\alpha x_2} - e^{\alpha x_1}} \quad b = \frac{y_2 e^{\alpha x_2} - y_1 e^{\alpha x_1}}{e^{\alpha x_2} - e^{\alpha x_1}} \tag{6}$$

The coordinates y_1, y_2, x_1, x_2 pertain to the points depicted in the Fig. 8, points A and B. Point $A(x_1, y_1)$ is the point where the flaring of the slot line starts. Simulations have shown that for a fixed length and width of the antenna, the optimum return loss was achieved when the curvature of the taper was closest to a round shape [10]. For the antenna length, the simulations have shown agreement with claims found in literature [10]: while it doesn't directly influence the return loss, it does influence the directivity of the antenna. In this work, in order to keep a minimum footprint of the Vivaldi antenna, the length of the antenna was reduced. The rationale of reducing the length was based on acceptable return loss levels $(-10\,\mathrm{dB})$, and not the actual directivity of the antenna. This might seem as defying the purpose of designing a very directional antenna, however this design decision had to be made in the favor of lessened footprint.

The choice of the substrate was made after assessing effects both on the operation of the antenna and that of the metamaterial. While it is convenient to have a substrate with a large dielectric constant
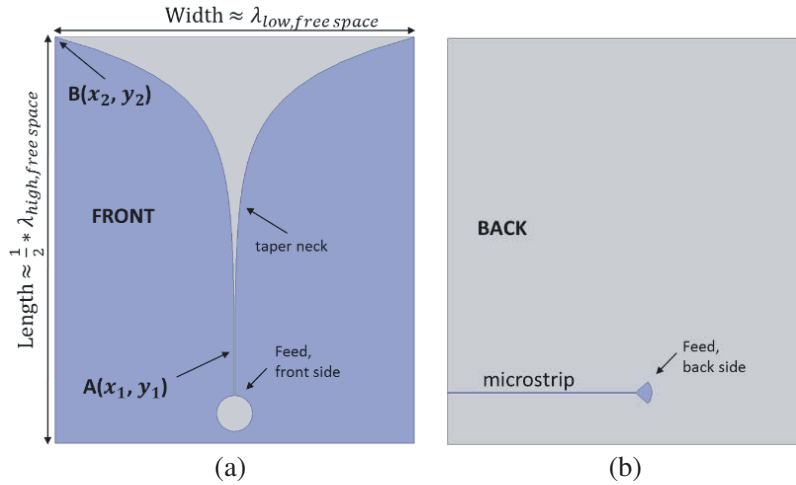
Figure 8. Vivaldi antenna coplanar design: Metallic flares and microstrip feed line represented with blue and substrate represented in light grey, front side in (a) and back side in (b). $\lambda_{low,freespace}$ represents the wavelength corresponding the lower frequency limit in the bandwidth and $\lambda_{high,freespace}$ represents the wavelength corresponding the higher frequency limit in the bandwidth.
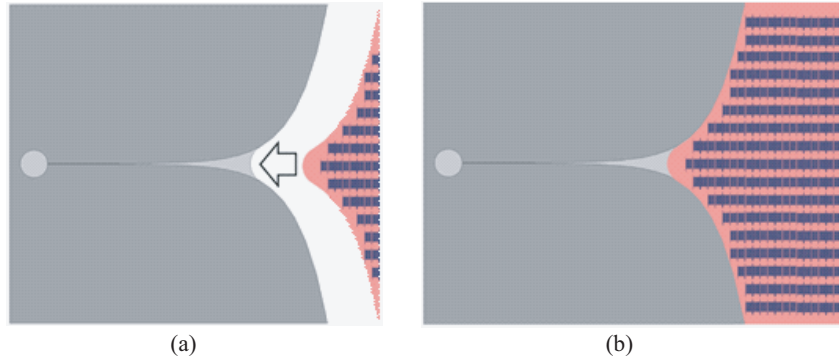

Figure 9. (a) Metamaterial fitted in the Vivaldi antenna aperture; (b) An additional metamaterial segment is added, in order to enhance the desired effect.

such that the antenna size is reduced, the same is not true for the design of the metamaterial. Given that the metamaterial has an anisotropic design, the value of the dielectric constant had be chosen such that it doesn't negatively affect operation of the metamaterial in any direction, as it was shown in the previous section.

Due to the very small size of the interior meanders of the final MwM structure, a PCB fabrication method couldn't be used for the metamaterials, therefore the whole systems couldn't be printed in one piece. The system had to be fabricated in 2 pieces, and subsequently assembled as shown in Fig. 9. The metamaterial was inserted into the aperture of the antenna is depicted in Fig. 9. This is only a proof of concept, the actual assembly of antenna and metamaterial was not achieved experimentally at this point in the project.

4. METAMATERIAL: NONRESONANT MATERIAL

The results presented in this section are preliminary HFSS simulations results. The idea is based on that of Gradient Index Lens. This design is still in the proof of concept stage and an analytical approach based on the construction and operation of a GRIN lens was not established at this stage of the work. A comparative analysis between 3 antennas is presented: a Vivaldi antenna, a metamaterial enhanced
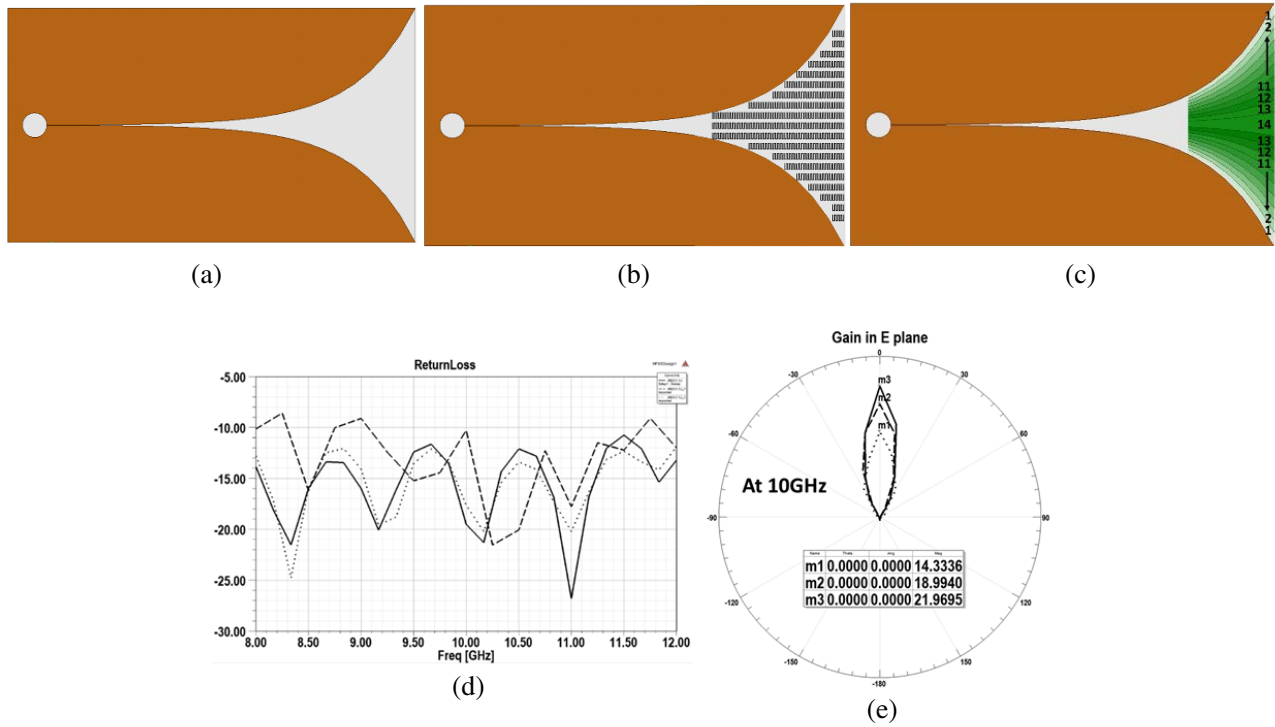
(a)   (b)   (c)

(d)

(e)

Figure 10. Geometries (top view) of the 3 cases analyzed. (a) The original Vivaldi antenna as designed by the B. Zhou et al. group [2]; (b) The metamaterial enhanced Vivaldi antenna as designed by the B. Zhou et al. group [13]; (c) The all-dielectric metamaterial Vivaldi antenna, where the dielectric material in between the apertures of the antenna varies from 14 in the middle to 1; (d) The return loss for all 3 cases: The original Vivaldi antenna (a) with dotted line, the metamaterial enhanced Vivaldi antenna using meander structures (b) with dashed line and the all-dielectric metamaterial (c) with black continuous line. Shown in (e) is the gain in the E plane for one frequency point only, $f = 10$ GHz, for all 3 cases: (a) The original Vivaldi antenna with dotted line; (b) The metamaterial enhanced Vivaldi antenna using meander structures with dashed line and (c) the all-dielectric metamaterialwith black continuous line.

Vivaldi antenna, a dielectric metamaterial enhanced Vivaldi antenna. The 3 antennas compared are depicted in Fig. 10. The antenna design parameters were the same ones used in the work of Zhou etal. [13]. A recent publication [14] describes a similar application, with a different design for the unit cell and a different operation frequency range.

As depicted in Fig. 10(c) the all-dielectric metamaterial inserted in the aperture of the antenna is composed of long segments, each of which has a different dielectric permittivity: the middle segment has the highest dielectric permittivity, $\varepsilon_r = 14$, and the following segments have a dielectric permittivity decreasing gradually until the segments reach the antenna flares. This construction creates the following effect: the wave velocity, defined simply by $v_{effective} = \frac{c}{n}$, where c is the speed of light and n is the index of refraction of the medium, of the wave travelling in the middle segment will travel slower than in the original case. Therefore, it will travel in phase with the wave travelling closer to the flares of the antenna. In other words, the graded index material lens is a lens which is collecting a wave with diverging profile and transforming it into a much more focused wave. Another way of understanding this effect is by comparing it with a fiber optic constructed with a graded index: the center part has a higher index of refraction, such that the beam is "trapped" and travelling in the core of the fiber optics. This shows a very good return loss for the all-dielectric metamaterial Vivaldi design, which is very close to that of the original Vivaldi antenna (dotted line in Fig. 10(d)).

A comparison between the three (3) antenna designs is presented at the frequency $f = 10$ GHz. The best gain is achieved by the all-dielectric metamaterial Vivaldi antenna. Even though losses haven't been
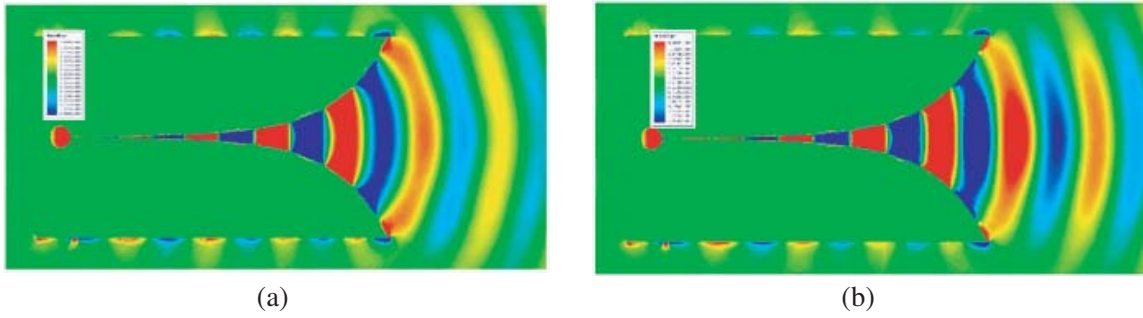
(a)   (b)

Figure 11. (a) E_y component of the electric field for the original Vivaldi antenna; (b) And for the all-dielectric metamaterial enhanced Vivaldi antenna.

added to this model, it is to be expected that the losses will not decrease the performance dramatically. It is to be expected that the gain will be at the same value as in the case of the Vivaldi antenna with meanders in the aperture, for the frequency of interest and a broader frequency interval as well. These results are preliminary and therefore the material used for the graded dielectric metamaterial are ideal, meaning no loss has been included in these simulations. To be noted is the fact that these materials are isotropic. The lensing effect of the graded index material is depicted in Fig. 11, where a snapshot of the E_y component of the electric field is shown. The wave front energy is concentrated in the middle portion of the axial trajectory, due to the graded material arrangement. The all-dielectric metamaterial Vivaldi antenna design has a few notable advantages:

- Since the metamaterial is not composed of a resonating structures, the bandwidth of operation and the gain is significantly improved.
- The losses issues associated with the use of metallic resonating structures are eliminated.
- The power handling capabilities of the system is improved since the metamaterial is composed of non-resonating structures. The risk of damaging the metallic resonant structures which compose the metamaterial is eliminated.

A potential candidate for the substrate is Rogers material Duroid 6010. The dielectric permittivity of Duroid 6010 material is $\varepsilon_r = 10.2$. This is not ideal, since in the preliminary simulations the middle segment is a material with a dielectric permittivity $\varepsilon_r = 14$. This will be addressed in future research.

The graded index will be achieved by a laser micromachining procedure. Sub wavelength holes will be drilled in the substrate material, in such a way that the desired effective permittivity, as depicted in Fig. 10(c) will be achieved. This procedure is what defines the all-dielectric material: a material composed of subwavelength "meta-atoms", which is this case will be tiny, subwavelength apertures, drilled in the dielectric material which serves as substrate for the Vivaldi antenna. The segment in the middle will contain no holes but as we move away from the center, the dielectric segments will be perforated with increasingly more holes, such that the graded all-dielectric material is mimicked. Just like the case of the meander resonating structures, the metamaterial will be embedded within the area between the antenna flares.

5. CONCLUSION

In this work, an anisotropic zero index material is designed, and a potential application is presented. The application is towards RF antenna design. Results presented are from simulation work done using HFSS software from Ansys. The method of reducing the footprint of the unit cell of the metamaterial was introduced and described. An alternative method of achieving a similar and potentially improved result is to use a non-resonant material instead, and the proof of concept for this method is described. Fabrication of the antenna was achieved with standard PCB fabrication methods, however the nanofabrication of the metamaterial is still in process. Experimental results will be presented in future work.

ACKNOWLEDGMENT

REFERENCES

1. Ziolkowski, R. W., "Metamaterials: The early years in the USA," *EPJ Appl. Metamat.*, Vol. 1, No. 5, 2014, DOI: 10.1051/epjam/2014004.

2. Alu, A., M. G. Silveirinha, A. Salandrino, and N. Engheta, "Epsilon-near-zero metamaterials and electromagnetic sources: Tailoring the radiation phase pattern," *Phys. Rev. B*, Vol. 75, 155410, Arpil 2007.

3. Yang, Y., Y. Wang, and A. E. Fathy, "Design of compact Vivaldi antenna arrays for UWB see through wall applications," *Progress In Electromagnetics Research*, Vol. 82, 401–418, 2008.

4. Gibson, P. J., "The Vivaldi aerial," *9th European Microwave Conference*, IEEE, 1979, DOI: 10.1109/EUMA.1979.332681.

5. Ambhore, V. B. and A. P. Dhande, "An overview on properties, parameter consideration and design of meandering antenna," *International Journal of Smart Sensors and Ad Hoc Networks*, Vol. 1, No. 4, 2012, ISSN No. 22248-9738.

6. Das, A., S. Dhar, and B. Gupta, "Lumped circuit model analysis of meander line antennas," *11th Mediterranean Microwave Symposium (MMS)*, 2011.

7. Warnagiris, T. J. and T. J. Minardo, "Performance of a meandered line as an electrically small transmitting antenna," *IEEE Transactions on Antennas and Propagation*, Vol. 46, No. 12, December 1998.

8. Popescu, A.-S., T. Rexhepi, I. Bendoym, A. Golovin, and D. T. Crouse, "UHf metamaterial enhanced antenna," *META'15, the 6th International Conference on Metamaterials, Photonic Crystals and Plasmonics*, New York, N.Y., 2015.

9. Chen, X., T. M. Grzegorczyk, B.-I. Wu, J. Pacheco, Jr., and J. A. Kong, "Robust method to retrieve the constitutive effective parameters of metamaterials," *Phys. Rev. E*, Vol. 70, 016608, July 26, 2004.

10. Nevrly, J., "Design of Vivaldi antenna," Diploma Thesis, Czech Technical University, Czech Republic, 2007.

11. Zinieris, M. M., R. Sloan, and L. E. Davis, "A broadband microstrip-to-slot-line transition," *Microwave and Optical Technology Letters*, Vol. 18, No. 5, August 1998.

12. Schuppert, B., "Microstrip/slotline transitions: Modeling and experimental investigation," *IEEE Transcations on Microwave Theory and Techniques*, Vol. 36, No. 8, August 1988.

13. Zhou, B., H. Li, X. Zou, and T.-J. Cui, "Broadband and high-gain planar Vivaldi antennas based on inhomogeneous anisotropic zero-index metamaterials," *Progress In Electromagnetics Research*, Vol. 120, 235–247, 2011.

14. Bhaskar, M., E. Johari, Z. Akhter, and M. J. Akhta, "Gain enhancement of the Vivaldi antenna with band notch characteristics using zero-index metamaterial," *Microwave and Optical Technology Letters*, Vol. 58, No. 1, 233–238, January 2016.